HHS Public Access

Author manuscript

J Am Chem Soc. Author manuscript; available in PMC 2023 May 28.

Published in final edited form as:

J Am Chem Soc. 2022 September 28; 144(38): 17651–17660. doi:10.1021/jacs.2c07225.

Subcellular Delivery of Hydrogen Sulfide Using Small Molecule Donors Impacts Organelle Stress

Annie K. Gilbert,

Michael D. Pluth*

Department of Chemistry and Biochemistry, Institute of Molecular Biology, Knight Campus for Accelerating Scientific Impact, Materials Science Institute, University of Oregon, Eugene, Oregon, 97403, USA.

Abstract

Hydrogen sulfide (H_2S) is an endogenously produced gaseous signaling molecule with important roles in regulating organelle function and stress. Because of its high reactivity, targeted delivery of H_2S using small molecule H_2S donors has garnered significant interest to minimize off-target effects. Although mitochondrially-targeted H_2S donors, such as AP39, have been reported previously and exhibit significantly higher potency than non-targeted donors, the expansion of targeted H_2S delivery to other subcellular organelles remains largely absent. To fill this key unmet need, we report a library of organelle-targeted H_2S donors that localize H_2S delivery to specific subcellular organelles, including the Golgi apparatus, lysosome, endoplasmic reticulum, and mitochondria. We measured H_2S production in vitro from each donor, confirmed the localization of H_2S delivery using organelle-specific H_2S responsive fluorescent probes, and demonstrated enhanced potency of these targeted H_2S donors in providing protection against organelle-specific stress. We anticipate this class of targeted H_2S donors will enable future studies of subcellular roles of H_2S and the pathways by which H_2S alleviates subcellular organelle stress.

Graphical Abstract

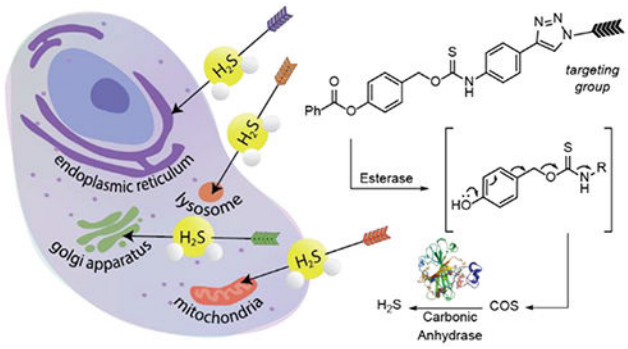

*Corresponding Author: pluth@uoregon.edu.

Supporting Information. Cell imaging studies, NMR spectra. This material is available free of charge via the Internet at http://pubs.acs.org.

Introduction

Site specific labeling or delivery to subcellular organelles provides a powerful method to affect subcellular machinery and processes. Much like different cell types play fundamental roles in biological structure, function, and assembly, different subcellular organelles carry out specific tasks required for cellular function. For example, the endoplasmic reticulum (ER) is essential for the assembly of proteins; the Golgi apparatus packages these proteins and transports them; the lysosome digests cellular waste; and the mitochondria provide energy to exert these functions. Malfunction of any of these organelles can result in disease. Mitochondrial dysfunction and resulting oxidative stress are linked to a variety of diseases such as Parkinson's disease,[1] type 2 diabetes,[2] and cardiovascular diseases.[3] Unfolded protein buildup results in ER stress, which can lead to neurological diseases like Alzheimer's disease and amyotrophic lateral sclerosis (ALS).[4] The Golgi apparatus is additionally involved in neurological diseases where Golgi fragmentation has been observed in neurons of patients with Alzheimer's disease, ALS, and Creutzfeldt-Jakob disease.[5] This relationship between organelle dysfunction and disease motivates the development of both research tools and therapeutic approaches that can help resolve specific organelle stress and aid in treating different diseases.

One such candidate is hydrogen sulfide (H_2S), an endogenously produced gaseous signaling molecule with important roles in regulating organelle function and stress. H_2S regulates mitochondrial biogenesis and oxidative stress,[6] attenuates ER stress in a variety of disease states,[7] and protects against Golgi stress by regulating intracellular Ca^{2+} levels.[8] Several of these effects are initiated through persulfidation of cysteine residues on proteins, which is an oxidative posttranslational modification stemming from H_2S oxidation to form persulfide and polysulfide intermediates that can subsequently undergo transpersulfidation.[9] Subcellular production of H_2S is moderated by three main enzymes including by cystathionine γ-lyase (CSE) and cystathionine β-synthase (CBS), which are generally localized in the cytosol, and 3-mercaptopyruvate sulfur transferase (3-MST), which is localized in the mitochondria. There is also evidence that CBS and CSE are not solely confined to the cytosol but rather localize in various organelles under certain conditions. For example, CBS has been shown to accumulate in the mitochondria in liver ischemia,[10] and both CBS and CSE can be transported to the nucleus upon modification by small ubiquitin-like modifier (SUMO) proteins.[11] Localization of these enzymes could be Nature's way of directing H_2S to the site of therapeutic need while reducing off-target effects. Developing chemical tools that can mimic this enzymatic localization of H_2S production could be one way to better understand subcellular roles of H_2S and investigate potential therapeutic effects of subcellular H_2S delivery.

Current strategies to investigate subcellular roles of H_2S include the use of chemical probes to visualize H_2S distribution,[12–18] regulation of CSE expression, and administration of exogenous sources of H_2S. Inorganic sulfide salts are often used as exogenous sources of H_2S but produce a large bolus of H_2S upon dissolving in water. This approach is not compatible with investigating subcellular H_2S effects as large amounts of these salts are required to observe any physiological effects and excess H_2S can lead to different biological outcomes due to off-target effects. To address these challenges of H_2S delivery, small

molecule donors have been developed to control the rate of H_2S release and localization of H_2S delivery.[19] H_2S donors can be tuned to react with specific analytes or environments at the site of therapeutic interest to produce H_2S or contain targeting groups to help localize delivery.

Few organelle-targeted H_2S donors have been developed, all of which target H_2S delivery to either the mitochondria or the lysosome (Figure 1a).[20–24] AP39, which is targeted to the mitochondria by a pendant triphenylphosphonium cation, is the most well-established targeted H_2S donor and exhibits significantly higher potency in promoting antioxidant and cytoprotective effects than non-targeted donors.[20] This high potency has made AP39 an attractive donor for investigating the therapeutic effects of H_2S. For example, AP39 has demonstrated promising therapeutic effects in ischemia injury, with AP39 treatment resulting in protection against myocardial reperfusion injury, and neuroprotective activity in brain ischemia models.[25–26] Additionally, AP39 has demonstrated protective roles in Alzheimer's disease (AD) where AP39 attenuated special memory deficits and inhibited brain atrophy in a mice AD model.[27] All these conditions heavily involve mitochondrial function and reactive oxygen species production, which suggests the mitochondria-targeting feature of AP39 could be important in promoting these therapeutic effects. Also targeting the mitochondria, HSD-B releases H_2S in response to reactive oxygen species, and was demonstrated to provide cytoprotection in a hypoxia/reoxygenation injury model in H9c2 cardiomyocytes. Two donors with lysosomal targeting groups have also been reported. UTS-2, which releases H_2S after thiol-mediated cleavage of the trisulfide, was demonstrated to localize to the lysosome and show minimal cytotoxicity. Lyso-pHTCM was demonstrated to provide increased H_2S release in acidic environments, but was not investigated in cellular environments. Despite evidence of other subcellular roles of H_2S, the expansion of targeted H_2S delivery to other organelles remains largely absent. In addition, whether subcellular targeting to other organelles can provide a more general approach to increase H_2S donor potency and to inform on local concentration requirements to generate biological outcomes remains an open question.

To address this key unmet need, we developed a library of organelle targeted H_2S donors using a caged thiocarbamate scaffold. Caged thiocarbamates (TCMs) are highly tunable H_2S donors that undergo an activatable 1,6-elimination to release carbonyl sulfide (COS), which is rapidly hydrolyzed by the ubiquitous enzyme carbonic anhydrase (CA) to produce H_2S.[28] Within the last decade, several examples of TCMs, as well as others approaches,[29–31] have been developed including those activated by light,[32–34] cysteine,[35] mildly acidic environments,[36] reactive oxygen species,[37] and esterases.[38–39] Here, we appended known organelle-targeted groups onto the esterase-activated TCM scaffold to localize H_2S delivery within specific subcellular regions (Figure 1b), providing a set of chemical tools to investigate subcellular H_2S effects. Due to the reactivity of H_2S, we hypothesized that targeting H_2S delivery within the cell to the area of therapeutic need would significantly enhance the efficacy of small molecule H_2S donors in resolving organelle stress.

Results and Discussion

Donor Design

To investigate the effects of subcellular H_2S delivery, we prepared a library of organelle-targeted caged thiocarbamate COS/H_2S donors. The caged thiocarbamate (TCM) scaffold is highly tunable and modular, which allows for simple attachment of targeting groups. We chose to use an esterase-activated thiocarbamate due to the widespread distribution of esterases throughout the cell, which should enable activation and COS production in diverse cellular environments. Different CA isoforms have been reported previously to be distributed throughout the cell including the matrix compartment of the mitochondria,[40] the lysosome,[41] the membrane of the ER,[42] the Golgi apparatus,[43] and the cytosol.[44] This ubiquitous distribution of CA should enable conversion of COS into H_2S regardless of the subcellular location of COS delivery. Although early work with esterase-activated thiocarbamates showed cytotoxicity in BEAS 2B human lung epithelial cells, related work with increased ester steric bulk or thiocarbamate isomers showed high biocompatibility in other cell lines.[39, 45] Building from these prior insights, we selected the phenyl ester thiocarbamate scaffold because of its low cytotoxicity, moderate release rate, and ease of installation.

To localize H_2S delivery to the mitochondria, lysosome, endoplasmic reticulum (ER), and Golgi apparatus, we appended known organelle targeting groups onto the thiocarbamate scaffold using azide/alkyne click chemistry. This approach has the added benefit of generating a triazole linkage between the donor and targeting group, which is significantly more resistant to cleavage than the commonly-used ester linkage in AP39. We used the well-established triphenylphosphonium and morpholine groups to target the mitochondria and lysosome, respectively. We used the *p*-toluenesulfonamide group, which binds potassium ATP channels on the membrane of the ER, to target the ER.[16] Lastly, we used a phenylsulfonamide group to target the Golgi apparatus due to its affinity for cyclo-oxygenase-2, which is maximally present in the Golgi apparatus of cancerous cells.[15, 46] Both of the sulfonamide-based targeting groups have been used previously to localize small molecule probes to these corresponding organelles.[15–16, 46]

Synthesis

To prepare the donors, we first synthesized 4-ethynl aryl isothiocyanate (**2**) by treating 4-ethynyl aniline with 1,1′-thiocarbonyldiimidazole. The thiocarbamate alkyne coupling partner (**TCM alkyne**) was prepared by coupling 4-(hydroxylmethyl)phenyl benzoate (**1**) and **2** in the presence of DBU (Scheme 1). Azides of the organelle-targeted groups were prepared according to literature procedures.[47–51] The azide targeting groups were appended to the **TCM alkyne** using a copper catalyzed azide-alkyne cycloaddition reaction with copper sulfate and sodium ascorbate in the presence of *tris*((1-benzyl-4-triazolyl)methyl)amine (TBTA). In our hands, the Cu-catalyzed click reaction required significant optimization, likely due to coordination of the sulfur-containing thiocarbamate to the Cu catalyst. We also found that the TBTA ligand often co-eluted with the thiocarbamate products, which required careful chromatographic separation of the product. Despite these

challenges, this route allows for an efficient and modular approach to attaching different targeting groups to COS/H_2S releasing motifs.

H_2S-Release Measurements—After preparing the library of organelle-targeted donors, we next evaluated H_2S release in the presence of porcine liver esterase (PLE) and carbonic anhydrase (CA) using an H_2S-selective electrode. For each targeted donor, we measured the H_2S release using the TCM (50 μM) in PBS (10 mM, pH 7.4) containing PLE (5 U mL^{-1}), and CA (25 μg mL^{-1}) under nitrogen over the course of 60 min. All targeted donors exhibited H_2S production in the presence of both CA and PLE (Figure 2). Over the course of 60 min, we observed 9–30% H_2S release efficiency, depending on the donor targeting groups. These release efficiencies are above those for AP39 (~10% over 24 h).[52] We observed that the sulfonamide based TCMs (**ERTCM** and **GolgiTCM**) exhibited lower efficiencies of H_2S release compared to **MitoTCM** and **LysoTCM**. We hypothesized that this decrease in H_2S production could be due to potential coordination of the sulfonamide targeting group to the Zn(II) site in CA. Despite the decreased efficiency for these two donors, the H_2S release is comparable with that of AP39 and can be used to increase H_2S levels in live cells (*vide infra*).

Live-Cell Imaging of Localized H_2S Delivery—We next evaluated the localization of H_2S delivery from the targeted donors using live-cell fluorescent imaging. To visualize and confirm H_2S production within live cells, we prepared the organelle-targeted H_2S-responsive fluorescent probes Mito-HS,[18] Na-H_2S-ER,[16] Lyso-AFP,[17] and Golgi-NH,[15] which target the mitochondria, ER, lysosome, and Golgi apparatus, respectively (Scheme 2). We note that prior cell imaging studies with AP39 used to support mitochondrial localization were performed with a non-targeted coumarin-azide fluorescent probe. Although a strong correlation between a non-targeted probe and a targeted dye provides strong evidence for donor specificity, there are several challenges with this approach that are difficult to overcome with slow releasing H_2S donors. We chose to use organelle-targeted fluorescent H_2S probes because H_2S is membrane permeable and could disperse throughout the cell once produced if not trapped in the local area of delivery. Furthermore, non-targeted H_2S probes could diffuse throughout the cell after reacting with H_2S and complicate direct observation of where H_2S delivery was localized. With the targeted probes in hand, we next imaged each targeted TCM in the presence of an organelle-targeted probe and commercial organelle-targeted dye.

To investigate the subcellular localization of H_2S release from targeted donors, we first incubated HeLa cells were incubated with the desired probe (Mito-HS, Lyso-AFP, Na-H_2S-ER, or Golgi-NH) and a complementary organelle marker dye (MitoTracker™, LysoTracker™, ER-Tracker™, or BODIPY™ TR Ceramide) for 30 min. After washing with PBS (pH 7.4, 10 mM), the cells were then incubated for 1 hour with either a targeted TCM (**MitoTCM**, **LysoTCM**, **ERTCM**, or **GolgiTCM**) or the non-targeted **TCM alkyne** as a control compound. As shown in Figure 2, a bright fluorescent response indicating H_2S production was observed with only 200 nM of targeted TCM, whereas the vehicle treatment had minimal fluorescence (Figure 3, Figures S2–S5). Notably, these results support that organelle targeted delivery allows for a significantly lower

donor concentration required to produce a visible turn-on response when compared to previously reported cell imaging experiments of non-targeted small molecule H_2S donors (50–100 μM).[35, 37–38, 45, 53–55] Furthermore, the fluorescent response for each targeted donor overlapped with the organelle marker dyes with high Pearson's coefficients further confirming localization, (**MitoTCM**/Mito-HS/MitoTracker™: 0.96, **LysoTCM**/Lyso-AFP/LysoTracker™: 0.94, **ERTCM**/Na-H_2S-ER/ERTracker™: 0.95, **GolgiTCM**/Golgi-NH/BODIPY™ TR Ceramide: 0.92).

To confirm that the observed turn-on fluorescent response was due to the organelle-targeting character of the TCMs, we next imaged the **TCM alkyne** donor alongside the targeted TCMs as a non-targeted control compound. Treatment with **TCM alkyne** resulted in significantly lower fluorescence than all targeted TCMs except for **LysoTCM** (Figure 4). This observation corroborates our hypothesis that appending directing groups onto the H_2S donor scaffold enables localization of H_2S delivery, but also suggests that non-targeted TCMs (and potentially other small molecule H_2S donors) may also accumulate in the lysosome. Considering the mildly acidity of the lysosome (pH 4.5 – 5.5) and the pK_a of H_2S (7.4), about 99% of H_2S released within the lysosome should be in the protonated and gaseous form (H_2S vs HS^-). Because the diprotic form of H_2S is membrane permeable, H_2S released within the lysosome would likely diffuse out of this organelle and into the cytoplasm, which would also be consistent with the unconfined fluorescence response typically observed with non-targeted donors. Moreover, lysosomal accumulation of H_2S donors could also contribute to the higher concentrations required to observe cellular H_2S production and to produce physiological effects than with non-targeted H_2S donors.

To demonstrate that H_2S release from targeted donors was specific to the targeted organelle, we also performed a separate cell imaging experiment in which we compared the response of mitochondrially-targeted Mito-HS probe, in the presence of **MitoTCM**, AP39 (a known mitochondrially-targeted H_2S donor), and **ERTCM** (Figure 5). Both **MitoTCM** and AP39 had comparable fluorescence responses as expected, but a minimal fluorescence response was observed for **ERTCM**. This diminished fluorescence in the presence of **ERTCM** further demonstrates the specificity of H_2S delivery with the targeted TCMs as H_2S production is enhanced only in the designated region of interest.

Cell Proliferation Experiments

Having confirmed the subcellular H_2S delivery and localization from the targeted TCMs, we next investigated the ability of these donors to protect against specific subcellular stress. We incubated H9C2 rat cardio myoblasts with Monensin, a known Golgi stressor, and varying concentrations of **GolgiTCM**. To evaluate the ability of **GolgiTCM** to protect against Golgi stress-induced cell death, we assessed the cell viability after 19 h of incubation using a Cell Counting Kit-8 (CCK-8). As shown in Figure 6, we observed a dose-dependent rescue of cell viability in the presence of **GolgiTCM**. These protective effects were observed at concentrations as low as 200 nM of **GolgiTCM**, whereas non-targeted sources of H_2S (**TCM alkyne** and NaSH) demonstrated no rescue of cell viability within the same range of concentration (1 μM). These results highlight the potency of localized H_2S delivery in resolving organelle-specific stress. To test whether the protective effective

of **GolgiTCM** was due to Golgi-targeted H_2S delivery, we additionally investigated the ability of **MitoTCM** and **LysoTCM** to protect cells against Golgi stress-induced cell death. Whereas **MitoTCM** resulted in the same rescue of cell viability as **GolgiTCM**, **LysoTCM** further decreased the cell viability at the same concentration. H_2S has previously been reported to induce cell death via lysosomal destabilization, albeit in primary mouse cortical neurons and likely through ionotropic glutamate receptor activation.[56] Although we observed H_2S production by each donor with cellular imaging, the COS hydrolysis activity of different CA isoforms throughout the cell have not been investigated and therefore the differences in cell protection could also be a result of COS versus H_2S effects. Further study of COS hydrolysis by different CA isoforms and the development of chemical probes to study COS production in cells are needed to help distinguish the effects of COS from H_2S. From these results, we hypothesize that H_2S can provide cytoprotective effects against Golgi stress through multiple pathways throughout the cell and we anticipate organelle-targeted sources of H_2S will enable investigation of these specific pathways. Furthermore, the localization of H_2S can result in contrasting effects depending on the subcellular organelle which highlights the significance of targeted delivery of H_2S.

Conclusions

We prepared the first library of organelle targeted H_2S donors to increase the available tools for investigating the subcellular effects of H_2S. These donors can be prepared using a modular click chemistry approach to append different targeting groups onto an esterase-activated TCM scaffold. Appending directing groups onto TCMs enabled subcellular localization of H_2S delivery, which was confirmed using live-cell fluorescent imaging and targeted H_2S-responsive probes. We also observed lysosomal localization of non-targeted TCM donors, which could help explain the higher concentrations required to produce physiological effects with non-targeted donors, further highlighting the importance of targeting H_2S delivery. We demonstrated that the organelle targeted donors have enhanced potency in protecting cells against organelle-specific stress. When compared to other small signaling gases like nitric oxide (NO), H_2S is sometimes thought to have a lower biological relevance due to the higher concentrations necessary to generate biological effects (apart from mitochondria-targeted delivery by AP39). This work demonstrates that substantially lower levels of H_2S can produce biological effects if H_2S delivery is directed to a specific site of therapeutic interest. Moreover, these benefits of targeting are observed in other organelles beyond the mitochondria. We anticipate this class of targeted TCMs will enable future studies of H_2S activity within specific organelles and provide new opportunities to investigate therapeutic effects of H_2S in diseases associated with specific organelle stress.

Experimental Section

Methods and Materials

Reagents were purchased from Sigma-Aldrich, Tokyo Chemical Industry (TCI), Fisher Scientific, Combi-Blocks, and VWR and used directly as received. Silica gel (SiliaFlash F60, Silicycle, 230−400 mesh) and preparatory TLC plates (SiliaPlate Prep TLC, Silicycle, 1000 μm thickness) was used for column chromatography. Deuterated solvents were

purchased from Cambridge Isotope Laboratories (Tewksbury, Massachusetts, USA). ^{1}H, $^{31}P\{^{1}H\}$, and $^{13}C\{^{1}H\}$ NMR spectra were recorded on Bruker 500 MHz and 600 MHz NMR instruments. Chemical shifts are reported in ppm relative to residual protic solvent resonances for ^{1}H and $^{13}C\{^{1}H\}$ NMR spectra. Mass spectrometric measurements were performed by the University of Illinois, Urbana Champaign MS facility or on a Xevo Waters ESI LC/MS instrument. H_2S electrode data were acquired with a World Precision Instruments (WPI) ISO-H2S-2 sensor connected to a TBR4100 Free Radical Analyzer or a Unisense H_2S Microsensor Sulf-100 connected to a Unisense Microsensor Multimeter. All air-free manipulations were performed under an inert atmosphere using standard Schlenk techniques or an Innovative Atmospheres N_2-filled glovebox.

H_2S Electrode Materials and Methods

Phosphate buffered saline (PBS) tablets (1X, CalBioChem) were used to make buffered solutions (PBS, 140 mM NaCl, 3 mM KCl, 10 mM phosphate, pH 7.4) in Millipore water. Buffer solutions were sparged with N_2 and stored in an N_2-filled glovebox. Carbonic anhydrase (CA) from bovine erythrocytes (≥3,500 W/A units/mg) and porcine liver esterase (PLE, ≥15 U/mg) was obtained from Sigma-Aldrich. A 10 mg/mL CA stock solution and a 1000 U/mL PLE stock solution was prepared in deoxygenated buffer (PBS, 10 mM, pH 7.4) in a glovebox immediately prior to use. Thiocarbamate stock solutions were prepared in an N_2-filled glovebox in DMSO and stored at −25 °C until immediately before use.

General Procedure for H_2S Electrode Experiments

Scintillation vials containing 20.0 mL of phosphate buffer (10 mM, pH 7.4) were prepared in an N_2-filled glovebox. The CA stock solution (50 μL, 10 mg/mL) and PLE stock solution (100 μL, 1000 U/mL) were injected into the vials. Outside of the glove box, the WPI/Unisense electrode was inserted into the vial with a split-top septum. The measured current was allowed to equilibrate before starting the experiment. With moderate stirring, the thiocarbamate stock solution (100 μL, 10 mM in DMSO) was injected and H_2S release was monitored using the electrode.

Cell Imaging

HeLa cells (ATCC CCL-2) were cultured in Dulbecco's modified Eagle's medium (DMEM) supplemented with 10% fetal bovine serum (FBS) and 1% penicillin/streptomycin at 37 °C under 5% CO_2. Poly-D-lysine coated glass-bottom imaging dishes (MatTek) were seeded with HeLa cells at 10,000 cells/cm^2 overnight. The cells were then washed and incubated with an H_2S-responsive fluorescent probe (Mito-HS, Lyso-AFP, Na-H_2S-ER, or Golgi-NH) and a commercial organelle-targeted dye (MitoTracker, LysoTracker, ER-Tracker, or BODIPY TR Ceramide) in FBS-free DMEM for 30 min. Cells were then washed with PBS and incubated with either a targeted TCM (**MitoTCM**, **LysoTCM**, **ERTCM**, or **GolgiTCM**), **TCM alkyne**, or vehicle (DMSO, 0.5%) in FBS-free DMEM for 60 min prior to being washed with PBS and imaged in FluoroBrite DMEM. Imaging was performed in replicate on a Leica DMi8 fluorescent microscope using DIC for bright field imaging and CY5 and GFP filter cubes for fluorescence imaging. Image workup was done in LAS X and Pearson's Coefficients were calculated in FIJI.[57]

Cell Viability Experiments

H9C2 cells (ATCC) were cultured in Dulbecco's modified Eagle's medium (DMEM) supplemented with 10% fetal bovine serum (FBS) and 1% penicillin/streptomycin at 37 °C under 5% CO_2. Cells were seeded at 10,000 cells/well in a 96-well plate overnight, then washed and incubated in FBS-free DMEM containing Monensin (0.5, 1, 2, and 3 μM) and incubated for 19 h. Cells were then washed with PBS, and a CCK-8 solution (1:10 in FBS-free DMEM) was added to each well. The cells then were incubated for 1–2 h at 37 °C under 5% CO_2. The absorbance at 450 nm was measured using a microplate reader, and the cell viability was measured and normalized to the vehicle group. Upon selection of the optimal Golgi stressor concentration, cells were treated with vehicle control or 1 μM/3 μM Monensin in the presence or absence of various concentrations of **GolgiTCM**, **TCM alkyne**, or NaSH for 19 h. Cell viability was accessed using the CCK-8 assay as described above. Results are expressed as mean ± SD (n = 12). P values were calculated using a Student's t test in Excel compared to DMSO alone.

Synthesis

1-Ethynyl-4-isothiocyanatobenzene (2).—4-Ethynylaniline (0.50 g, 4.3 mmol, 1.0 equiv) was dissolved in anhydrous CH_2Cl_2 (20 mL). The reaction was cooled to 0 °C, and then a solution of 1,1′-thiocarbonyldiimidazole (0.761 g, 4.27 mmol, 1.0 equiv) in CH_2Cl_2 (5 mL) was added dropwise. The reaction mixture was stirred at 0 °C for 1 h, warmed to room temperature, and stirred for an additional 1 h. The crude reaction mixture was evaporated and purified by column chromatography (12–100% EtOAc/Hexanes) to isolate a white solid (0.585 g, 86%). ^{1}H NMR (600 MHz, $CDCl_3$) δ: 7.46 (d, J = 8.6 Hz, 2H), 7.17 (d, J = 8.5 Hz, 2H), 3.16 (s, 1H). ^{13}C{^{1}H} NMR (151 MHz, $CDCl_3$) δ: 137.1, 133.5, 131.8, 125.9, 121.3, 82.6, 79.3. HRMS (ES+ TOF) (m/z): $[M]^+$ calc'd for C_9H_5NS 159.01427; found 159.01439.

TCM alkyne.: 4-(Benzoyloxy)benzenemethanol (**1**) (201 mg, 0.876 mmol, 1.0 equiv) and **2** (146 mg, 0.920 mmol 1.05 equiv) were combined in anhydrous THF (10 mL) under N_2. The reaction mixture was cooled to 0 °C before adding DBU (148 μL, 0.964 mmol, 1.10 equiv). The reaction mixture was warmed to room temperature and stirred for 4 h. The reaction was quenched with brine (10 mL) and extracted with EtOAc (3 × 10 mL). The combined organic layers were dried over anhydrous $MgSO_4$, filtered, evaporated, and purified by silica column chromatography (2–32% EtOAc/Hexanes) to obtain the product as a white solid (157 mg, 46%). ^{1}H NMR (500 MHz, DMSO-d_6, 60 °C) δ: 11.25 (s, 1H), 8.14 (d, J = 6.8 Hz, 1H), 7.75 (t, J = 7.4 Hz, 1H), 7.62 (t, J = 7.8 Hz, 2H), 7.56 (d, J = 8.3 Hz, 2H), 7.44 (d, J = 8.3 Hz, 2H), 7.33 (d, J = 8.5 Hz, 2H), 5.61 (s, 2H), 4.03 (s, 1H). ^{13}C{^{1}H} NMR (126 MHz, DMSO, 60 °C) δ: 187.0, 164.3, 150.3, 138.4, 133.7, 133.2, 131.8, 129.5, 129.3, 128.8, 128.7, 121.8, 121.7, 117.7, 83.0, 80.0, 70.5. TOF MS (ASAP+) (m/z): $[M + H]^+$ calc'd for $C_{23}H_{18}NO_3S$, 388.1007; found, 388.1015.

Azide Targeting Groups

MitoN$_3$ was prepared according to previous reports.[47–48]

(6-Bromohexyl)triphenylphosphonium bromide.—1,6-Dibromohexane (0.94 mL, 6.1 mmol, 1.0 equiv) and triphenylphosphonium bromide (0.532 g, 2.03 mmol, 0.33 equiv) were combined in MeCN (35 mL) and refluxed for 12 h. After cooling to room temperature, the solvent was evaporated, and the crude mixture was dissolved in DI water (10 mL) and extracted with EtOAc (3 × 20 mL). The crude product was purified by column chromatography (10% MeOH/CH_2Cl_2) to afford a white powder (1.07 g, 34%). ^{1}H NMR (500 MHz, DMSO-d_6) δ: 7.90 (m, 3H), 7.83 – 7.72 (m, 12H), 3.62 – 3.51 (m, 2H), 3.49 (t, J = 6.7 Hz, 2H), 1.74 (p, J = 6.8 Hz, 2H), 1.62 – 1.44 (m, 4H), 1.39 (m, 2H). ^{13}C{H} NMR (126 MHz, DMSO-d_6) δ: 134.9 (d, J = 2.9 Hz), 133.6 (d, J = 10.1 Hz), 130.2 (d, J = 12.3 Hz), 118.5 (d, J = 85.8 Hz), 34.9, 31.8, 28.9 (d, J = 16.8 Hz), 26.7, 21.6 (d, J = 4.2 Hz), 20.2 (d, J = 50.0 Hz). ^{31}P{^{1}H} NMR (202 MHz, DMSO-d_6) δ: 24.03.

(6-Azidohexyl)triphenylphosphonium bromide.—(4-bromobutyl)triphenylphosphonium bromide (0.5 g, 1 mmol) was dissolved in EtOH/H_2O (1:1, 1.2 mL). NaN_3 (77 mg, 1.2 mmol, 1.2 equiv) was added, and the reaction mixture was shielded from light and heated to 100 °C overnight. The reaction mixture was cooled to room temperature, and the solvent was evaporated. The crude product was purified by column chromatography (10% MeOH/CH_2Cl_2) to afford a white solid (0.438 mg, 95%). ^{1}H NMR (600 MHz, $CDCl_3$) δ: 7.91 – 7.82 (m, 6H), 7.82 – 7.76 (m, 3H), 7.70 (m, 6H), 3.94 – 3.85 (m, 2H), 3.24 (t, J = 6.7 Hz, 2H), 1.72 (m, 2H), 1.63 (h, J = 8.1 Hz, 2H), 1.54 (m, 4H), 1.39 (m, 2H). ^{13}C{H} NMR (151 MHz, $CDCl_3$) δ: 135.1 (d, J = 3.0 Hz), 133.9 (d, J = 10.0 Hz), 130.6 (d, J = 12.6 Hz), 118.6 (d, J = 85.8 Hz), 51.3, 29.9 (d, J = 16.3 Hz), 28.6, 26.5, 22.8 (d, J = 49.7 Hz), 22.8 (d, J = 4.5 Hz). ^{31}P{H} NMR (202 MHz, $CDCl_3$) δ: 19.66.

LysoN$_3$ was prepared according to the reported procedures.[49]

Trifluoromethanesulfonyl azide (TfN$_3$).—NaN_3 (1.17 g, 18.0 mmol, 6.0 equiv) was added to water (3 mL) and CH_2Cl_2 (1.1 mL) and cooled to 0 °C. Once cooled, Tf_2O (0.5 mL, 3 mmol, 1.0 equiv) was added dropwise over 5 minutes to the reaction solution and stirred for an additional 2 h at 0 °C. The organic phase was separated, and the aqueous phase was extracted with CH_2Cl_2 (3 mL). The combined organic layers were washed with saturated aqueous $NaHCO_3$ (10 mL) and reserved for the next step.

4-(2-Azidoethyl)morpholine.—4-(2-Aminoethyl)morpholine (130 mg, 1.00 mmol, 1.0 equiv) was dissolved in CH_2Cl_2 (0.7 mL) and cooled to 0 °C. NEt_3 (0.42 mL, 3.0 mmol, 3.0 equiv) and a solution of $CuSO_4$•$5H_2O$ (13 mg, 0.050 mmol, 0.05 equiv) in water (0.17 mL) was added to the reaction mixture. The reserved solution of TfN_3 was added dropwise followed by addition of MeOH (0.7 mL). The reaction mixture was stirred at room temperature overnight, then quenched with saturated aqueous $NaHCO_3$ (10 mL), and extracted with CH_2Cl_2 (3 × 10 mL). The combined organic layers were washed with brine, dried over $MgSO_4$, and purified by column chromatography (5% MeOH/CH_2Cl_2). The product was isolated as a yellow solid (146 mg, 94%). ^{1}H NMR (500 MHz, $CDCl_3$) δ: 3.73 (t, J = 4.7 Hz, 4H), 3.37 (t, J = 6.0 Hz, 2H), 2.61 (t, J = 6.0 Hz, 2H), 2.52 (t, J = 4.6 Hz, 4H). ^{13}C{^{1}H} NMR (126 MHz, $CDCl_3$) δ: 66.7, 57.6, 53.6, 47.9.

ERN$_3$ was prepared according to the modified reported procedure.[50] 2-Chloroethaneamine HCl (0.40 g, 3.5 mmol, 1.0 equiv) was dissolved in water (4 mL). NaN_3 (0.682 g, 10.5 mmol, 3.0 equiv) was added, and then the reaction mixture was heated to 80 °C for 24 h. The reaction mixture was basified with NaOH (1 M) and then extracted with CH_2Cl_2 (3 × 2 mL). Sulfonyl chloride (0.667 g, 3.50 mmol, 1.0 equiv) was then added to the combined organic layers at room temperature. The resultant reaction mixture was stirred for 3 h, concentrated under vacuum, and purified by column chromatography (25% EtOAc/Hexanes). The product was isolated as a clear oil (0.301 g, 35%). ^{1}H NMR (500 MHz, $CDCl_3$) δ: 7.76 (d, J = 8.3 Hz, 2H), 7.32 (d, J = 8.0 Hz, 2H), 4.96 (t, J = 6.5 Hz, 1H), 3.40 (t, J = 5.7 Hz, 2H), 3.11 (q, J = 6.0 Hz, 2H), 2.43 (s, 3H). ^{13}C{^{1}H} NMR (126 MHz, $CDCl_3$) δ: 144.0, 136.9, 130.0, 127.2, 51.0, 42.5, 21.7.

GolgiN$_3$ was prepared according to the reported procedures.[49, 51] *4-(2-Azidoethyl)-benzenesulfonamide*. TfN_3 was freshly prepared according to the procedure above. 4-(2-Aminoethyl)benzenesulfonamide (201 mg, 1.00 mmol, 1.0 equiv) was dissolved in CH_2Cl_2 (3 mL) and MeOH (6 mL). The reaction mixture was cooled to 0 °C and then $CuSO_4$•$5H_2O$ (13 mg, 0.050 mmol, 0.05 equiv) was added. The freshly prepared TfN_3 was then added dropwise. The reaction mixture was stirred at room temperature for 16 h, and then the solvents were removed under vacuum. The crude product was redissolved in EtOAc, washed with brine, and dried over $MgSO_4$. The filtered and evaporated crude product was purified by column chromatography (10% MeOH/CH_2Cl_2). The product was isolated as a pale-yellow solid (177 mg, 78%). ^{1}H NMR (500 MHz, DMSO-d_6) δ: 7.76 (d, J = 7.9 Hz, 2H), 7.47 (d, J = 7.9 Hz, 2H), 3.62 (t, J = 7.1 Hz, 2H), 2.93 (t, J = 7.1 Hz, 2H). ^{13}C{^{1}H} NMR (126 MHz, DMSO-d_6) δ: 142.6, 142.4, 129.3, 125.7, 51.1, 34.1.

General Procedure for the Synthesis of Targeted Thiocarbamates

The **TCM alkyne** (1.0 equiv), azide coupling partner (1.08 equiv), and TBTA (1.0 equiv) were dissolved in CH_2Cl_2 (2.6 mL). An aqueous solution of sodium ascorbate (2.0 equiv) and $CuSO_4$•$5H_2O$ (2.0 equiv) was prepared and mixed thoroughly to generate an orange suspension containing copper (I) catalytic species. The copper (I) solution was added to the CH_2Cl_2 reaction mixture, and the resultant mixture was shielded from light and stirred vigorously at room temperature for 1 h. Water (10 mL) was then added, and the mixture was extracted with CH_2Cl_2 (3 × 10 mL). The combined organic phases were dried over $MgSO_4$, filtered, and evaporated under reduced pressure. The reaction was then purified by column chromatography.

MitoTCM was prepared with MitoN_3 and TCM alkyne according to the general procedure above and purified by column chromatography (10% MeOH/DCM) to isolate a white solid (13 mg, 68%). ^{1}H NMR (600 MHz, DMSO-d_6) δ: 11.21 (s, 1H), 8.46 (s, 1H), 8.14 (d, J = 6.6 Hz, 2H), 7.97 – 7.85 (m, 3H), 7.85 – 7.70 (m, 17H), 7.62 (t, J = 7.8 Hz, 2H), 7.58 (d, J = 8.1 Hz, 2H), 7.34 (d, J = 8.3 Hz, 2H), 5.62 (s, 2H), 4.36 (t, J = 7.0 Hz, 2H), 3.62 – 3.38 (m, 2H), 1.83 (p, J = 7.1 Hz, 2H), 1.53 (m, 4H), 1.41 – 1.22 (m, 2H). ^{13}C{^{1}H} NMR (151 MHz, DMSO-d_6) δ: 187.0, 164.3, 150.3, 145.6, 134.6 (d, J = 3.2 Hz), 133.8, 133.3 (d, J = 10.2 Hz), 130.0 (d, J = 12.3 Hz), 129.5, 129.3, 128.8, 128.7 (d, J = 2.9 Hz), 128.4, 125.9, 125.1, 122.5, 121.7, 120.8, 118.6, 118.1, 49.1, 48.3, 28.9 (d, J = 3.3 Hz), 24.7, 21.4 (d, J = 4.3 Hz),

20.3 (d, J = 50.1 Hz). $^{31}P\{^{1}H\}$ NMR (202 MHz, DMSO) δ: 24.0. HRMS (ES+ TOF) (m/z): $[M]^+$ calcd for $C_{47}H_{44}N_4O_3SP$ 775.2872; found 775.2850.

LysoTCM was prepared with $LysoN_3$ and TCM alkyne according to the general procedure above with the following modifications: the reaction was run in the absence of TBTA for 16 h at room temperature. The reaction was worked up according to the generalized procedure above and purified by column chromatography (5% $MeOH/CH_2Cl_2$) to isolate a white solid (13 mg, 53%). ^{1}H NMR (600 MHz, DMSO-d_6) δ: 11.19 (s, 1H), 8.46 (s, 1H), 8.14 (d, J = 6.7 Hz, 2H), 7.80 (d, J = 7.9 Hz, 2H), 7.75 (t, J = 7.4 Hz, 1H), 7.61 (t, J = 7.8 Hz, 2H), 7.58 (d, J = 8.1 Hz, 2H), 7.33 (d, J = 8.5 Hz, 2H), 5.62 (s, 2H), 4.51 (t, J = 6.3 Hz, 2H), 3.68 – 3.48 (m, 4H), 2.81 (t, J = 6.4 Hz, 2H), 2.45 (t, J = 4.6 Hz, 4H). $^{13}C\{^{1}H\}$ NMR (151 MHz, DMSO) δ: 187.0, 164.3, 150.3, 145.5, 137.4, 133.8, 133.4, 129.5, 129.3, 128.8, 128.7, 127.4, 125.2, 122.5, 121.7, 121.2, 70.4, 65.9, 57.1, 52.8, 46.6. HRMS (ES+ TOF) (m/z): $[M+H]^+$ calcd for $C_{29}H_{30}N_5O_4S$ 544.2019; found 544.2014.

ERTCM was prepared with ERN_3 and TCM alkyne according to the general procedure above and purified by column chromatography (10% MeOH/DCM) to isolate a white solid (10 mg, 25%). ^{1}H NMR (600 MHz, DMSO-d_6) δ: 11.29 – 11.07 (m, 1H), 8.36 (s, 1H), 8.14 (d, J = 6.9 Hz, 2H), 7.83 – 7.69 (m, 5H), 7.69 – 7.59 (m, 5H), 7.58 (d, J = 8.2 Hz, 2H), 7.34 (d, J = 6.2 Hz, 4H), 5.62 (s, 2H), 4.44 (t, J = 6.1 Hz, 2H), 3.39 – 3.26 (m, 2H), 2.33 (s, 3H). $^{13}C\{^{1}H\}$ NMR (151 MHz, DMSO) δ: 205.9, 187.0, 164.3, 150.4, 145.6, 142.5, 137.3, 133.8, 133.4, 129.5, 129.4, 129.3, 128.8, 128.7, 127.3, 126.2, 125.2, 122.5, 121.7, 121.2, 49.2, 42.2, 30.3, 20.6. HRMS (ES+ TOF) (m/z): $[M+H]^+$ calcd for $C_{32}H_{30}N_5O_5S_2$ 628.1688; found 628.1688.

GolgiTCM was prepared with $GolgiN_3$ and TCM alkyne according to the general procedure above with the following modifications: the reaction was run in the absence of TBTA and sonicated for 1 h before stirring at room temperature overnight. The reaction was worked up according to the generalized procedure above and purified by column chromatography (5% $MeOH/CH_2Cl_2$) to isolate a white solid (14 mg, 36%). ^{1}H NMR (600 MHz, DMSO-d_6) δ: 11.19 (s, 1H), 8.46 (s, 1H), 8.14 (d, J = 6.9 Hz, 2H), 7.90 – 7.69 (m, 6H), 7.66 – 7.59 (m, 5H), 7.41 (d, J = 8.3 Hz, 2H), 7.33 (d, J = 8.5 Hz, 2H), 7.17 (s, 2H), 5.61 (s, 2H), 4.70 (t, J = 7.1 Hz, 2H), 3.32 (t, J = 7.2 Hz, 2H). $^{13}C\{^{1}H\}$ NMR (151 MHz, DMSO) δ: 187.1, 164.3, 150.3, 145.6, 142.4, 141.5, 133.8, 133.3, 129.5, 129.3, 128.9, 128.7, 127.3, 126.3, 125.5, 125.2, 122.5, 122.1, 121.7, 120.8, 70.4, 49.9, 34.9. HRMS (ES+ TOF) (m/z): $[M+H]^+$ calcd for $C_{31}H_{28}N_5O_5S_2$ 614.1523; found 614.1532.

Mito-HS was prepared according to the reported procedure.[18]

4-Bromo-1,8-napthalic anhydride (0.50 g, 1.8 mmol, 1.0 equiv) was dissolved in DMF (7.2 mL), and then a suspension of NaN_3 (0.178 g, 2.70 mmol, 1.5 equiv) in water (0.3 mL) was added. The reaction mixture was stirred vigorously for 5 h at room temperature and then poured into ice water to precipitate the product. The product was filtered off as a yellow solid (0.378 g, 88%).

(3-Ammoniopropyl)triphenyl phosphonium bromide (60 mg, 0.15 mmol, 1.0 equiv) and 4-azido-1,8-naphtalic anhydride (36 mg, 0.15 mmol, 1.0 equiv) were combined in MeOH

(7.5 mL) and NEt_3 (0.85 mL) was added. The reaction mixture was heated to reflux for 8 h, cooled to room temperature, and the solvents were removed under vacuum. The crude product was purified by column and then by using a preparatory TLC plate (10% MeOH/CH_2Cl_2) to yield 9.8 mg of product (11% yield). ^{1}H NMR (500 MHz, CD_3OD) δ 8.59 (d, *J* = 7.5 Hz, 1H), 8.57 (d, *J* = 8.0 Hz, 1H), 8.53 (d, *J* = 8.2 Hz, 1H), 7.93 – 7.69 (m, 19H), 7.67 (d, *J* = 8.0 Hz, 1H), 4.34 (t, *J* = 7.1 Hz, 2H), 3.70 – 3.53 (m, 2H), 2.15 (m, 2H).

Lyso-AFP was prepared according to the reported procedures.[14, 17] 4-Bromo-1,8-napthalic anhydride (120 mg, 0.43 mmol, 1.0 equiv) and 4-(2-aminoethyl)morpholine (57 μL, 0.434 mmol, 1.0 equiv) were combined in EtOH (15 mL) and heated to reflux for 3 h. The reaction mixture was cooled to room temperature and filtered to afford a yellow solid (58 mg, 69%). The resulting product (LysoBr) was carried forward without further purification. LysoBr (60.0 mg, 0.154 mmol, 1.0 equiv) was dissolved in DMF (3 mL). A solution of NaN_3 (18 mg, 0.28 mmol, 1.8 equiv) in H_2O (0.5 mL) was added dropwise. The reaction mixture was stirred at 100 °C for 8 h, then quenched with H_2O (10 mL) and extracted into CH_2Cl_2 (3 × 20 mL). The combined organic layers were washed with a 5% LiCl solution in H_2O (5 × 20 mL) and brine (1 × 20 mL), then dried over $MgSO_4$, filtered, and evaporated. The crude product was purified by column chromatography (5% MeOH/CH_2Cl_2) to isolate a yellow solid (13 mg, 23%). ^{1}H NMR (500 MHz, $CDCl_3$) δ: 8.64 (d, *J* = 7.3 Hz, 1H), 8.59 (d, *J* = 7.7 Hz, 1H), 8.46 (d, *J* = 8.4 Hz, 1H), 7.75 (t, *J* = 7.9 Hz, 1H), 7.48 (d, *J* = 8.1 Hz, 1H), 4.34 (t, *J* = 7.0 Hz, 2H), 3.68 (t, *J* = 4.7 Hz, 4H), 2.70 (t, *J* = 7.0 Hz, 2H), 2.60 (s, 4H).

Na-H_2S-ER was prepared according to the reported procedures.[16, 58] 4-Bromo-1,8-napthalic anhydride (51.4 mg, 0.215 mmol, 1.0 equiv) and *N*-(2-aminoethyl)-4-methylbenzenesulfonamide (60 mg, 0.28 mmol, 1.3 equiv) were combined in EtOH (0.5 mL) and heated to reflux. The reaction mixture was stirred for 3 h, then cooled to room temperature, filtered, and dried to give a white solid (67 mg, 66% yield). The benzenesulfonamide (66.7 mg, 0.141 mmol, 1.0 equiv) was combined with NaN_3 (45.8 mg, 0.705 mmol, 5.0 equiv) in 3 mL of DMF and stirred at 50 °C for 8 h. Water (10 mL) was added, and the reaction mixture was extracted with CH_2Cl_2 (3 × 20 mL), washed with 5 % LiCl (4 × 20 mL) and brine (1 × 20 mL), dried over $MgSO_4$, filtered, and evaporated. The crude product was purified by column chromatography (3:1 EtOAc/Hex) to isolate a yellow solid (12 mg, 20%). ^{1}H NMR (500 MHz, DMSO-d_6) δ: 8.50 (d, *J* = 7.3 Hz, 1H), 8.45 (t, *J* = 8.4 Hz, 2H), 7.87 (t, *J* = 8.0 Hz, 1H), 7.77 (d, *J* = 8.1 Hz, 1H), 7.73 (t, *J* = 6.3 Hz, 1H), 7.57 (d, *J* = 8.5 Hz, 2H), 7.22 (d, *J* = 7.9 Hz, 3H), 4.10 (t, *J* = 6.7 Hz, 3H), 3.08 (q, *J* = 6.5 Hz, 3H), 2.25 (s, 4H).

GolgiNH was prepared according to the reported procedures.[15] 4-Bromo-1,8-napthalic anhydride (478 mg, 2.00 mmol, 1.0 equiv) and sulfanilamide (344 mg, 2.00 mmol, 1.0 equiv) were dissolved in acetic acid (5 mL) and refluxed for 8 h. The reaction mixture was cooled to room temperature for 1 h, and the precipitate was filtered and dried to yield a grey solid (0.326 g, 38%). The crude product (GolgiBr) was carried over to the next step without further purification. GolgiBr (60.0 mg, 0.139 mmol, 1.0 equiv) and NaN_3 were dissolved in DMSO (3 mL) and stirred at 100 °C for 2 h. The reaction was quenched with H_2O and extracted into DCM (3 × 20 mL). The combined organic layers were washed with brine (20 mL), dried over $MgSO_4$, filtered, and evaporated. The crude product was purified by column

chromatography (75% EtOAc/Hex) to yield (9 mg, 16%). ^{1}H NMR (500 MHz, DMSO-d_6) δ: 8.57 (d, J = 7.3 Hz, 1H), 8.55 – 8.50 (m, 2H), 7.97 (d, J = 8.5 Hz, 2H), 7.96 – 7.90 (m, 1H), 7.83 (d, J = 8.0 Hz, 1H), 7.62 (d, J = 8.5 Hz, 2H), 7.51 (s, 2H).

Supplementary Material

Refer to Web version on PubMed Central for supplementary material.

ACKNOWLEDGMENT

Financial support was provided by the NIH (R01GM113030 to MDP) and the NSF (DGE-1842486 to AKG). Instrumentation for fluorescence microscopy is supported by the NSF (CHE-1531189). We thank Dr. Carolyn Levinn for initial work with related thiocarbamate alkyne synthesis and optimization.

REFERENCES

(1). Hauser DN; Hastings TG, Mitochondrial Dysfunction and Oxidative Stress in Parkinson's Disease and Monogenic Parkinsonism. Neurobiol. Dis 2013, 51, 35–42. [PubMed: 23064436]

(2). Rochette L; Zeller M; Cottin Y; Vergely C, Diabetes, Oxidative Stress and Therapeutic Strategies. Biochim. Biophys. Acta - Gen. Subjects 2014, 1840(9), 2709–2729.

(3). Siasos G; Tsigkou V; Kosmopoulos M; Theodosiadis D; Simantiris S; Tagkou NM; Tsimpiktsioglou A; Stampouloglou PK; Oikonomou E; Mourouzis K, Mitochondria and Cardiovascular Diseases—from Pathophysiology to Treatment. Annu. Translat. Med 2018, 6(12), 256.

(4). Roussel BD; Kruppa AJ; Miranda E; Crowther DC; Lomas DA; Marciniak SJ, Endoplasmic Reticulum Dysfunction in Neurological Disease. Lanced Neurol. 2013, 12(1), 105–118.

(5). Machamer CE, The Golgi Complex in Stress and Death. Front. Neurosci 2015, 9, 421. [PubMed: 26594142]

(6). Paul BD; Snyder SH; Kashfi K, Effects of Hydrogen Sulfide on Mitochondrial Function and Cellular Bioenergetics. Redox Biol. 2021, 38, 101772. [PubMed: 33137711]

(7). Wang H; Shi X; Qiu M; Lv S; Liu H, Hydrogen Sulfide Plays an Important Protective Role through Influencing Endoplasmic Reticulum Stress in Diseases. Int. J. Biol. Sci 2020, 16(2), 264. [PubMed: 31929754]

(8). Zhang Y; Wang Y; Read E; Fu M; Pei Y; Wu L; Wang R; Yang G, Golgi Stress Response, Hydrogen Sulfide Metabolism, and Intracellular Calcium Homeostasis. Antioxid. Redox Signal 2020, 32(9), 583–601. [PubMed: 31870162]

(9). Paul BD; Snyder SH, H_2S: A Novel Gasotransmitter That Signals by Sulfhydration. Trends Biochem. Sci 2015, 40(11), 687–700. [PubMed: 26439534]

(10). Teng H; Wu B; Zhao K; Yang G; Wu L; Wang R, Oxygen-Sensitive Mitochondrial Accumulation of Cystathionine B-Synthase Mediated by Lon Protease. Proc. Natl. Acad. Sci. USA 2013, 110(31), 12679–12684. [PubMed: 23858469]

(11). Agrawal N; Banerjee R, Human Polycomb 2 Protein Is a Sumo E3 Ligase and Alleviates Substrate-Induced Inhibition of Cystathionine B-Synthase Sumoylation. PloS one 2008, 3(12), e4032. [PubMed: 19107218]

(12). Montoya LA; Pluth MD, Organelle-Targeted H_2S Probes Enable Visualization of the Subcellular Distribution of H_2S Donors. Anal. Chem 2016, 88(11), 5769–5774. [PubMed: 27171507]

(13). Chen J; Zhao M; Jiang X; Sizovs A; Wang MC; Provost CR; Huang J; Wang J, Genetically Anchored Fluorescent Probes for Subcellular Specific Imaging of Hydrogen Sulfide. Analyst 2016, 141(4), 1209–1213. [PubMed: 26806071]

(14). Liu T; Xu Z; Spring DR; Cui J, A Lysosome-Targetable Fluorescent Probe for Imaging Hydrogen Sulfide in Living Cells. Organic Lett. 2013, 15(9), 2310–2313.

(15). Zhu H; Liu C; Liang C; Tian B; Zhang H; Zhang X; Sheng W; Yu Y; Huang S; Zhu B, A New Phenylsulfonamide-Based Golgi-Targeting Fluorescent Probe for H2S and Its Bioimaging Applications in Living Cells and Zebrafish. Chem. Commun 2020, 56(29), 4086–4089.

(16). Tang Y; Xu A; Ma Y; Xu G; Gao S; Lin W, A Turn-on Endoplasmic Reticulum-Targeted Two-Photon Fluorescent Probe for Hydrogen Sulfide and Bio-Imaging Applications in Living Cells, Tissues, and Zebrafish. Sci. Rep 2017, 7(1), 1–9. [PubMed: 28127051]

(17). Qiao Q; Zhao M; Lang H; Mao D; Cui J; Xu Z, A Turn-on Fluorescent Probe for Imaging Lysosomal Hydrogen Sulfide in Living Cells. RSC Adv. 2014, 4(49), 25790–25794.

(18). Wu Z; Liang D; Tang X, Visualizing Hydrogen Sulfide in Mitochondria and Lysosome of Living Cells and in Tumors of Living Mice with Positively Charged Fluorescent Chemosensors. Anal. Chem 2016, 88(18), 9213–9218. [PubMed: 27537069]

(19). Levinn CM; Cerda MM; Pluth MD, Activatable Small-Molecule Hydrogen Sulfide Donors. Antioxid. Redox Signal 2020, 32(2), 96–109. [PubMed: 31554416]

(20). Szczesny B; Módis K; Yanagi K; Coletta C; Le Trionnaire S; Perry A; Wood ME; Whiteman M; Szabo C, Ap39, a Novel Mitochondria-Targeted Hydrogen Sulfide Donor, Stimulates Cellular Bioenergetics, Exerts Cytoprotective Effects and Protects against the Loss of Mitochondrial DNA Integrity in Oxidatively Stressed Endothelial Cells in Vitro. Nitric oxide 2014, 41, 120–130. [PubMed: 24755204]

(21). Gilbert AK; Zhao Y; Otteson CE; Pluth MD, Development of Acid-Mediated H_2S/COS Donors That Respond to a Specific pH Window. J. Org. Chem 2019, 84(22), 14469–14475. [PubMed: 31479268]

(22). Zhang N; Hu P; Wang Y; Tang Q; Zheng Q; Wang Z; He Y, A Reactive Oxygen Species (Ros) Activated Hydrogen Sulfide (H2S) Donor with Self-Reporting Fluorescence. ACS Sensors 2020, 5(2), 319–326. [PubMed: 31913018]

(23). Mahato SK; Bhattacherjee D; Bhabak KP, The Biothiol-Triggered Organotrisulfide-Based Self-Immolative Fluorogenic Donors of Hydrogen Sulfide Enable Lysosomal Trafficking. Chem. Commun 2020, 56(56), 7769–7772.

(24). Chen Y; Zhao R; Tang C; Zhang C; Xu W; Wu L; Wang Y; Ye D; Liang Y, Design and Development of a Bioorthogonal, Visualizable and Mitochondria-Targeted Hydrogen Sulfide (H2S) Delivery System. Angew. Chem. Int. Ed 2022, 61(6), e202112734.

(25). Karwi QG; Bornbaum J; Boengler K; Torregrossa R; Whiteman M; Wood ME; Schulz R; Baxter GF, Ap39, a Mitochondria-Targeting Hydrogen Sulfide (H2S) Donor, Protects against Myocardial Reperfusion Injury Independently of Salvage Kinase Signalling. Br. J. Pharmacol 2017, 174(4), 287–301. [PubMed: 27930802]

(26). Pomierny B; Krzyżanowska W; Jurczyk J; Skórkowska A; Strach B; Szafarz M; Przejczowska-Pomierny K; Torregrossa R; Whiteman M; Marcinkowska M, The Slow-Releasing and Mitochondria-Targeted Hydrogen Sulfide (H2S) Delivery Molecule Ap39 Induces Brain Tolerance to Ischemia. Int. J. Mol. Sci 2021, 22(15), 7816. [PubMed: 34360581]

(27). Zhao F.-l.; Fang F; Qiao P.-f.; Yan N; Gao D; Yan Y, Ap39, a Mitochondria-Targeted Hydrogen Sulfide Donor, Supports Cellular Bioenergetics and Protects against Alzheimer's Disease by Preserving Mitochondrial Function in App/Ps1 Mice and Neurons. Oxid. Med. Cell. Longev 2016, 2016, 8360738. [PubMed: 27057285]

(28). Levinn CM; Cerda MM; Pluth MD, Development and Application of Carbonyl Sulfide-Based Donors for H_2S Delivery. Acc. Chem. Res 2019, 52(9), 2723–2731. [PubMed: 31390174]

(29). Powell CR; Foster JC; Okyere B; Theus MH; Matson JB, Therapeutic Delivery of H_2S Via COS: Small Molecule and Polymeric Donors with Benign Byproducts. Journal of the American Chemical Society 2016, 138(41), 13477–13480. [PubMed: 27715026]

(30). Kaur K; Enders P; Zhu Y; Bratton AF; Powell CR; Kashfi K; Matson JB, Amino Acid-Based H_2S Donors: *N*-Thiocarboxyanhydrides That Release H_2S with Innocuous Byproducts. Chem. Commun 2021, 57(45), 5522–5525.

(31). Khodade VS; Pharoah BM; Paolocci N; Toscano JP, Alkylamine-Substituted Perthiocarbamates: Dual Precursors to Hydropersulfide and Carbonyl Sulfide with Cardioprotective Actions. J. Am. Chem. Soc 2020, 142(9), 4309–4316. [PubMed: 32058717]

(32). Zhao Y; Bolton SG; Pluth MD, Light-Activated COS/H2S Donation from Photocaged Thiocarbamates. Organic Lett. 2017, 19(9), 2278–2281.

(33). Sharma AK; Nair M; Chauhan P; Gupta K; Saini DK; Chakrapani H, Visible-Light-Triggered Uncaging of Carbonyl Sulfide for Hydrogen Sulfide (H2S) Release. Organic Lett. 2017, 19(18), 4822–4825.

(34). Štacko P; Muchová L; Vítek L; Klán P, Visible to Nir Light Photoactivation of Hydrogen Sulfide for Biological Targeting. Organic Lett. 2018, 20(16), 4907–4911.

(35). Zhao Y; Steiger AK; Pluth MD, Cysteine-Activated Hydrogen Sulfide (H2S) Delivery through Caged Carbonyl Sulfide (COS) Donor Motifs. Chem. Commun 2018, 54(39), 4951–4954.

(36). Gilbert AK; Zhao Y; Otteson CE; Pluth MD, Development of Acid-Mediated H2S/COS Donors That Respond to a Specific pH Window. The Journal of organic chemistry 2019, 84(22), 14469–14475. [PubMed: 31479268]

(37). Zhao Y; Pluth MD, Hydrogen Sulfide Donors Activated by Reactive Oxygen Species. Angew. Chem. Int. Ed 2016, 55(47), 14638–14642.

(38). Chauhan P; Bora P; Ravikumar G; Jos S; Chakrapani H, Esterase Activated Carbonyl Sulfide/ Hydrogen Sulfide (H2S) Donors. Organic Lett. 2017, 19(1), 62–65.

(39). Steiger AK; Marcatti M; Szabo C; Szczesny B; Pluth MD, Inhibition of Mitochondrial Bioenergetics by Esterase-Triggered COS/H2S Donors. ACS Chem. Biol 2017, 12(8), 2117–2123. [PubMed: 28613823]

(40). Dodgson SJ; Forster R 2nd; Storey B; Mela L, Mitochondrial Carbonic Anhydrase. Proc. Natl. Acad. Sci. USA 1980, 77(9), 5562–5566. [PubMed: 6776540]

(41). Rikihisa Y, Ultrastructural Localization of Carbonic Anhydrase in Lysosomes. Anatom. Rec 1985, 211(1), 1–8.

(42). Ono Y; Ridderstråle Y; Forster R 2nd; Chu ZG; Dodgson S, Carbonic Anhydrase in the Membrane of the Endoplasmic Reticulum of Male Rat Liver. Proc. Natl. Acad. Sci. USA 1992, 89(24), 11721–11725. [PubMed: 1465389]

(43). Alvarez L; Fanjul M; Carter N; Hollande E, Carbonic Anhydrase Ii Associated with Plasma Membrane in a Human Pancreatic Duct Cell Line (Capan-1). J. Histochem. Cytochem 2001, 49(8), 1045–1053. [PubMed: 11457932]

(44). Tashian RE, Genetics of the Mammalian Carbonic Anhydrases. Advances Genet. 1992, 30, 321–356. [PubMed: 1456113]

(45). Levinn CM; Steiger AK; Pluth MD, Esterase-Triggered Self-Immolative Thiocarbamates Provide Insights into COS Cytotoxicity. ACS Chem. Biol 2019, 14(2), 170–175. [PubMed: 30640440]

(46). Wang H; He Z; Yang Y; Zhang J; Zhang W; Zhang W; Li P; Tang B, Ratiometric Fluorescence Imaging of Golgi H_2o_2 Reveals a Correlation between Golgi Oxidative Stress and Hypertension. Chem. Sci 2019, 10(47), 10876–10880. [PubMed: 32190242]

(47). Chen X; Khairallah GN; Richard A; Williams SJ, Fixed-Charge Labels for Simplified Reaction Analysis: 5-Hydroxy-1, 2, 3-Triazoles as Byproducts of a Copper (I)-Catalyzed Click Reaction. Tetrahedron Lett. 2011, 52(21), 2750–2753.

(48). Yang W; Chan PS; Chan MS; Li KF; Lo PK; Mak NK; Cheah KW; Wong MS, Two-Photon Fluorescence Probes for Imaging of Mitochondria and Lysosomes. Chem. Commun 2013, 49(33), 3428–3430.

(49). Peng B; Thorsell AG; Karlberg T; Schüler H; Yao SQ, Small Molecule Microarray Based Discovery of Parp14 Inhibitors. Angew. Chem. Int. Ed 2017, 56(1), 248–253.

(50). Fang L; Trigiante G; Crespo-Otero R; Philpott MP; Jones CR; Watkinson M, An Alternative Modular 'Click-Snar-Click'approach to Develop Subcellular Localised Fluorescent Probes to Image Mobile Zn2+. Org. Biomol. Chem 2019, 17(47), 10013–10019. [PubMed: 31621740]

(51). Chambers JM; Hill PA; Aaron JA; Han Z; Christianson DW; Kuzma NN; Dmochowski IJ, Cryptophane Xenon-129 Nuclear Magnetic Resonance Biosensors Targeting Human Carbonic Anhydrase. J. Am. Chem. Soc 2009, 131(2), 563–569. [PubMed: 19140795]

(52). Gerő D; Torregrossa R; Perry A; Waters A; Le-Trionnaire S; Whatmore JL; Wood M; Whiteman M, The Novel Mitochondria-Targeted Hydrogen Sulfide (H2S) Donors Ap123 and Ap39 Protect against Hyperglycemic Injury in Microvascular Endothelial Cells in Vitro. Pharmacol. Res 2016, 113, 186–198. [PubMed: 27565382]

(53). Zhao Y; Steiger AK; Pluth MD, Colorimetric Carbonyl Sulfide (COS)/Hydrogen Sulfide (H_2S) Donation from Γ-Ketothiocarbamate Donor Motifs. Angew. Chem 2018, 130(40), 13285–13289.

(54). Zhao Y; Cerda MM; Pluth MD, Fluorogenic Hydrogen Sulfide (H_2S) Donors Based on Sulfenyl Thiocarbonates Enable H_2S Tracking and Quantification. Chem. Sci 2019, 10(6), 1873–1878. [PubMed: 30842856]

(55). Zhao Y; Steiger AK; Pluth MD, Cyclic Sulfenyl Thiocarbamates Release Carbonyl Sulfide and Hydrogen Sulfide Independently in Thiol-Promoted Pathways. J. Am. Chem. Soc 2019, 141(34), 13610–13618. [PubMed: 31373809]

(56). Cheung NS; Peng ZF; Chen MJ; Moore PK; Whiteman M, Hydrogen Sulfide Induced Neuronal Death Occurs Via Glutamate Receptor and Is Associated with Calpain Activation and Lysosomal Rupture in Mouse Primary Cortical Neurons. Neuropharmacology 2007, 53(4), 505–514. [PubMed: 17692345]

(57). Schindelin J; Arganda-Carreras I; Frise E; Kaynig V; Longair M; Pietzsch T; Preibisch S; Rueden C; Saalfeld S; Schmid B; Tinevez J-Y; White DJ; Hartenstein V; Eliceiri K; Tomancak P; Cardona A, Fiji: An Open-Source Platform for Biological-Image Analysis. Nature Meth. 2012, 9(7), 676–682.

(58). Xu A; Tang Y; Lin W, Endoplasmic Reticulum-Targeted Two-Photon Turn-on Fluorescent Probe for Nitroreductase in Tumor Cells and Tissues. Spectrochim. Acta. A. Mol. Biomol. Spect 2018, 204, 770–776.

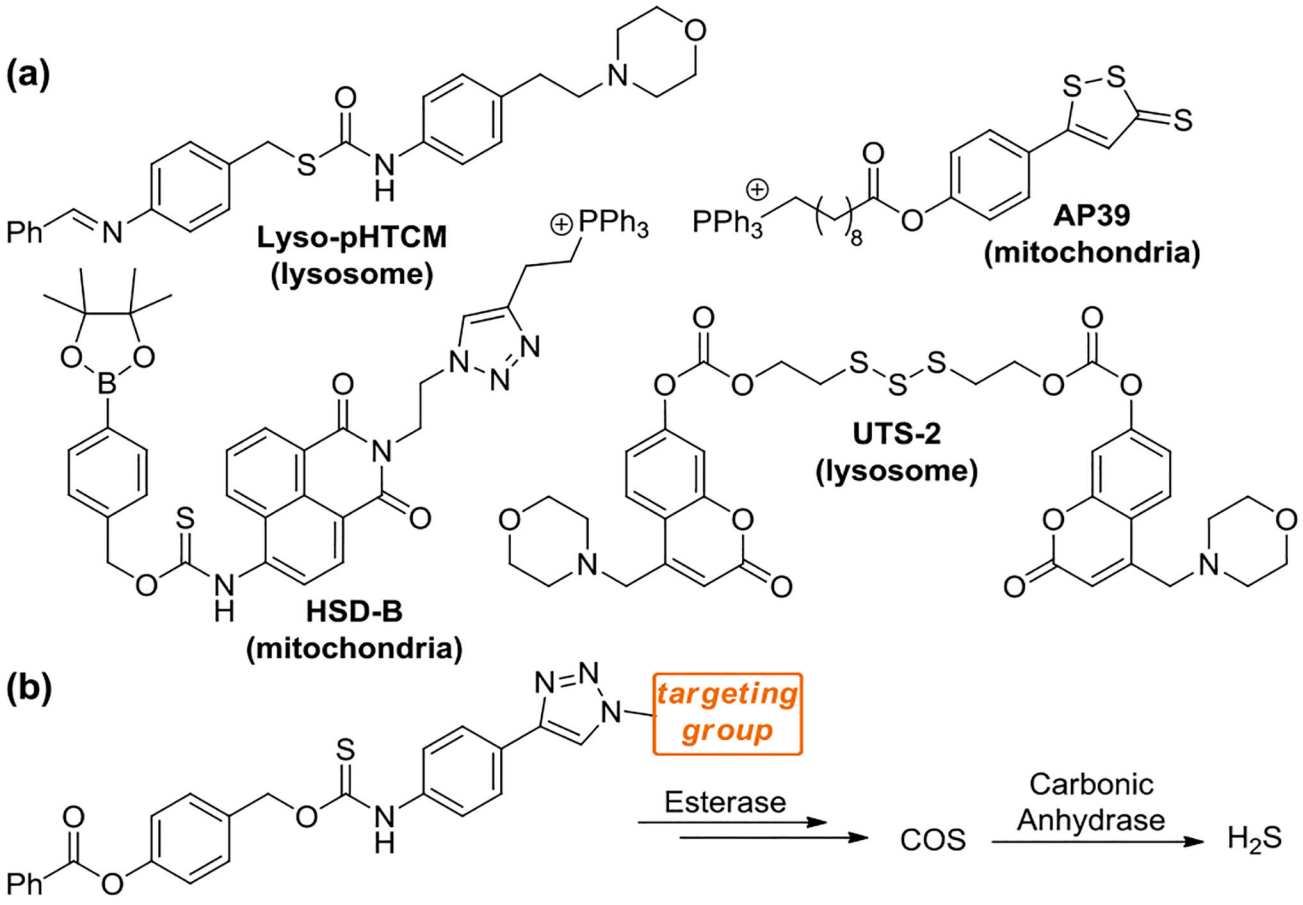

Figure 1.

(a) Current library of organelle-targeted donors with targeted organelle indicated below.

(b) Targeted delivery of carbonyl sulfide (COS)/H_2S via esterase-activated caged thiocarbamates.

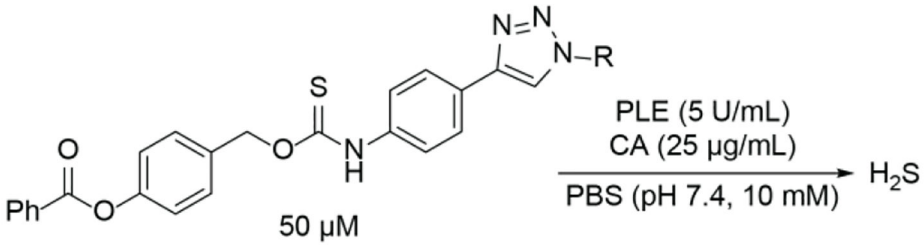

a)

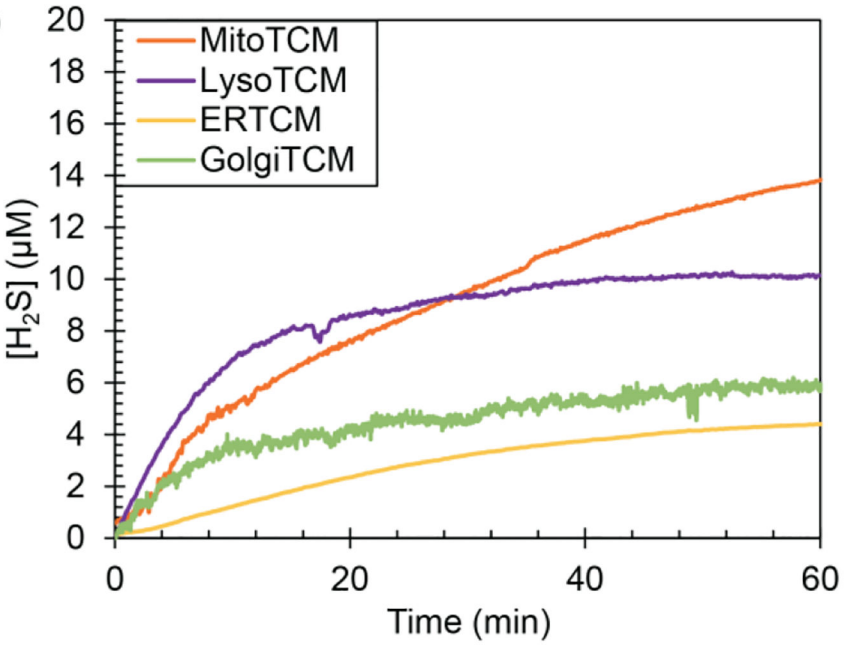

b)

Donor	Initial rate (μM s^{-1})	k_{obs} x10^{-4} (s^{-1})
MitoTCM	0.60 ± 0.07	4.4 ± 0.9
LysoTCM	0.9 ± 0.5	16 ± 5
GolgiTCM	0.7 ± 0.1	16 ± 5
ERTCM	0.11 ± 0.05	6.2 ± 0.3

Figure 2.

a) H_2S release from organelle targeted TCMs (50 μM) in the presence of PLE (5 U mL^{-1}) and CA (25 μg mL^{-1}) in PBS (10 mM, pH 7.4) using an H_2S-selective electrode. Experiments were performed in triplicate, and the release curves shown are the mean values (n = 3). b) Rates of H_2S release reported as initial rates (μM s^{-1}) and pseudo 1st-order rate constants (k_{obs}) with results expressed as mean ± S.E. (n = 3).

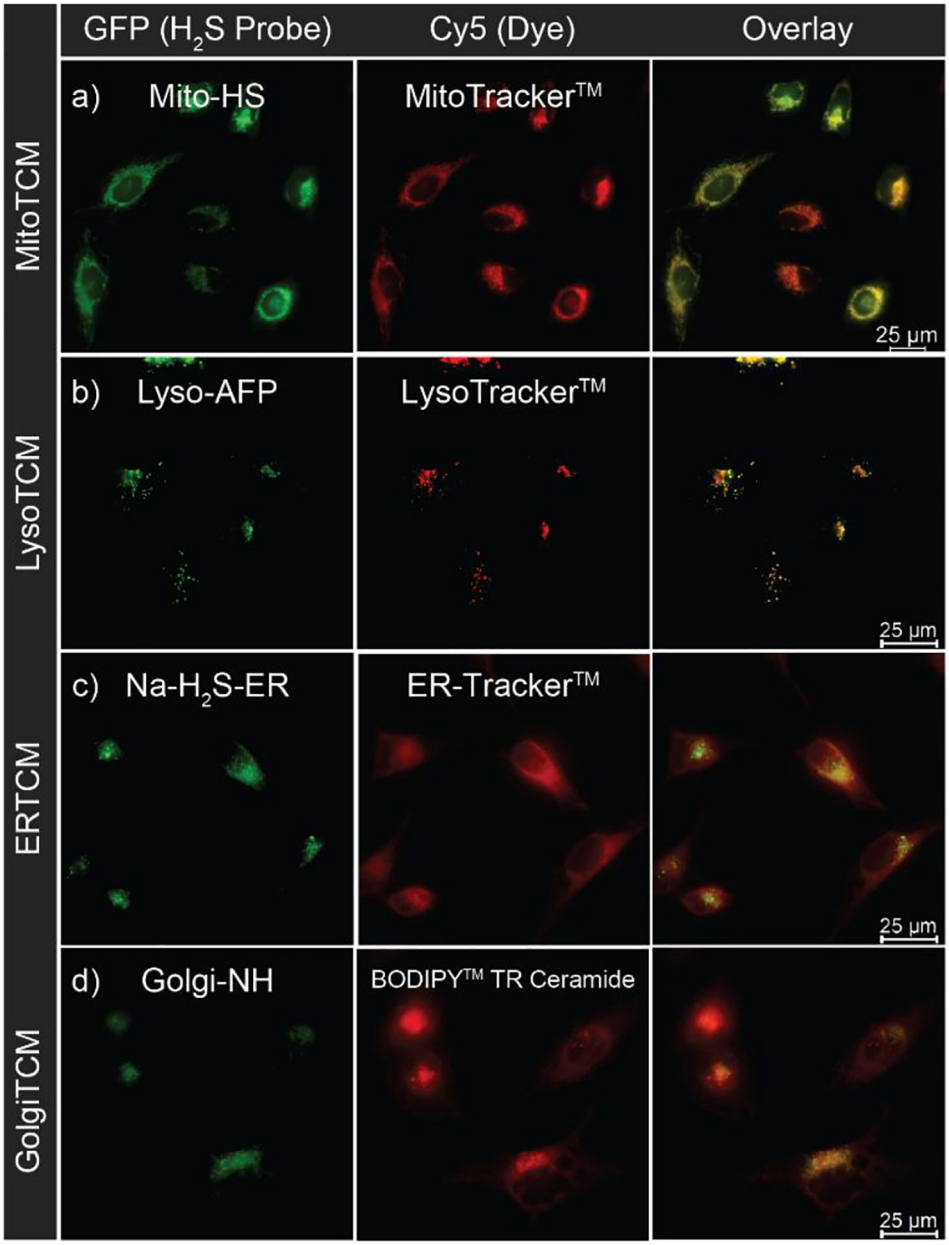

Figure 3.

Live-cell imaging of localized H_2S production in HeLa cells. (a) Mitochondria-localized H_2S delivery from **MitoTCM** (200 nM) in the presence of Mito-HS (10 μM) and MitoTracker™ (50 nM). (b) Lysosome-localized H_2S delivery from **LysoTCM** (200 nM) in the presence of Lyso-AFP (10 μM) and LysoTracker™ (50 nM). (c) ER-localized H_2S delivery from **ERTCM** (200 nM) in the presence of Na-H_2S-ER (10 μM) and ER-Tracker™ (1 μM). (d) Golgi-localized H_2S delivery from **GolgiTCM** (200 nM) in the presence of Golgi-NH (5 μM) and BODIPY™ TR Ceramide (2 μg/mL).

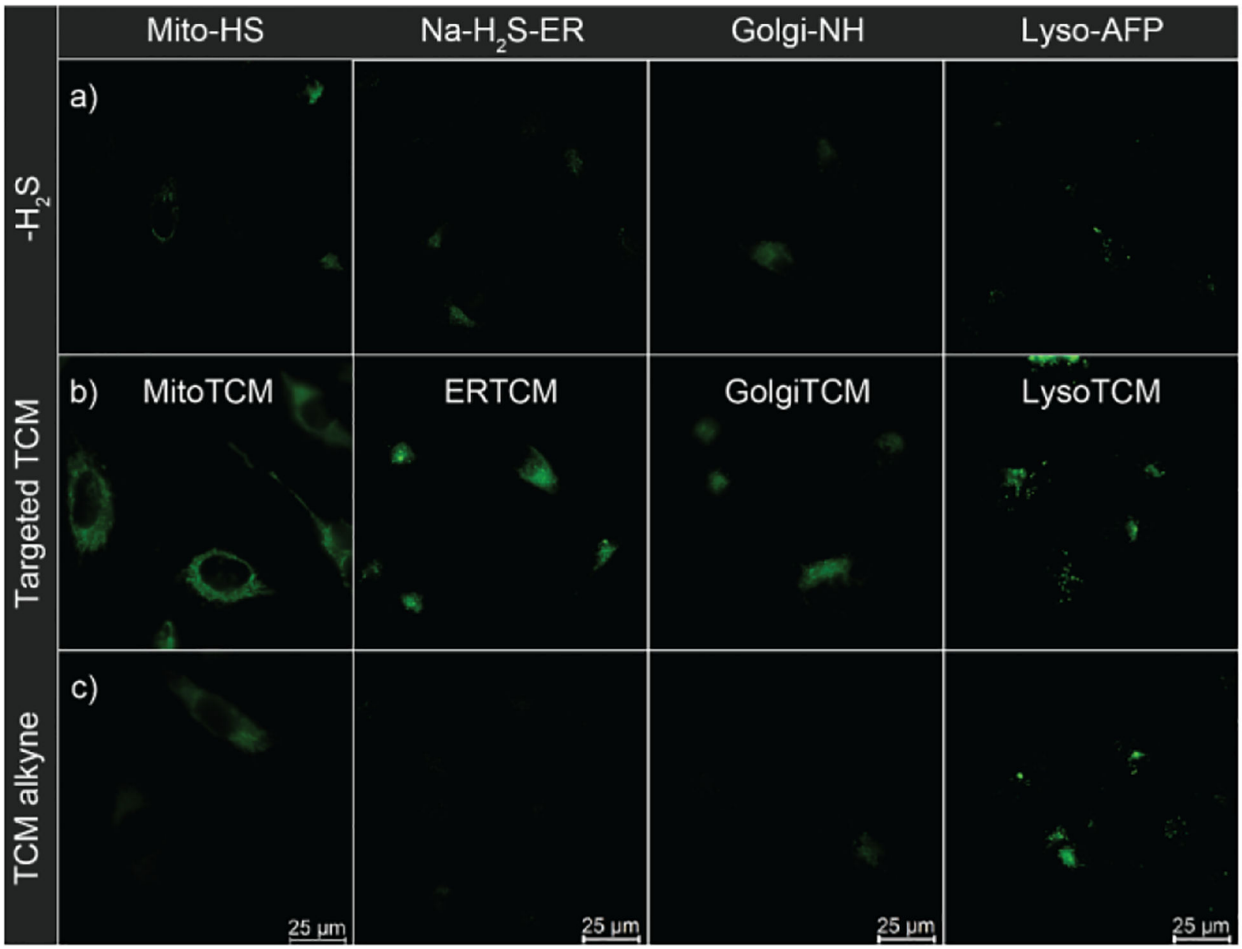

Figure 4.

Fluorescent turn-on response of targeted H_2S probes in the presence of targeted TCMs compared to non-targeted control (**TCM alkyne**). HeLa cells were treated with probe (5 μM Mito-HS, 10 μM Na-H_2S-ER, 5 μM Golgi-NH, or 10 μM Lyso-AFP) and (a) No exogenous H_2S (b) Targeted TCM (200 nM), or (c) **TCM alkyne** (200 nM).

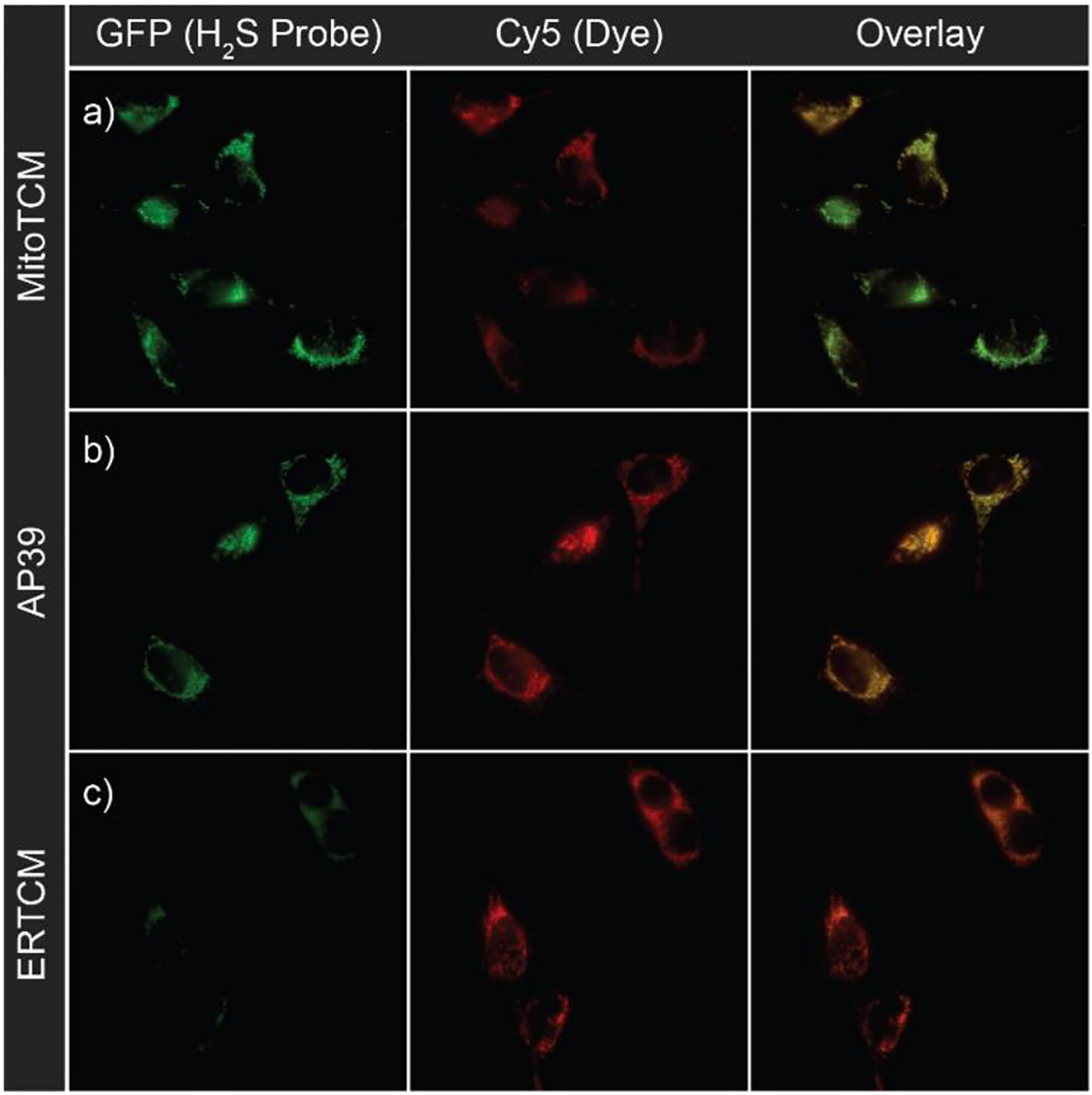

Figure 5.
Live-cell imaging of 200 nM (a) **MitoTCM** (b) AP39 and (c) **ERTCM** in the presence of Mito-HS (10 μM) and MitoTracker™ (50 nM).

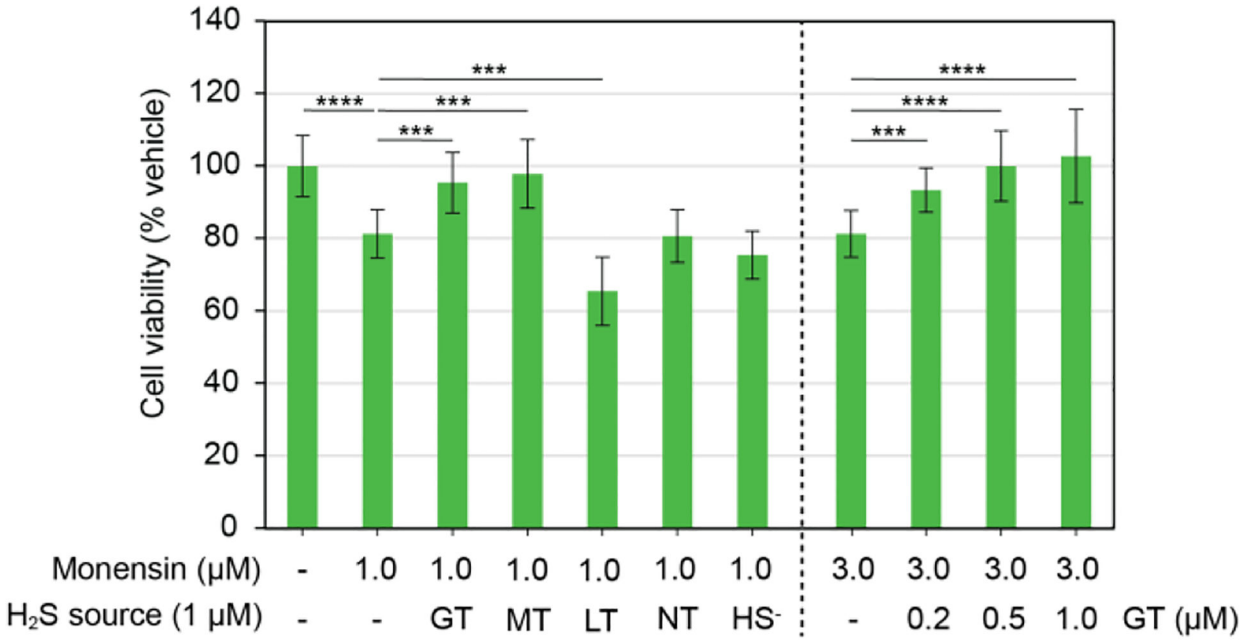

Figure 6.

GolgiTCM and **MitoTCM** protect against Golgi stress-induced cell death. H9C2 cells were treated with Monensin (1 or 3 μM) and either DMSO (0.5%), **GolgiTCM** (GT, 0.2, 0.5, or 1 μM), **MitoTCM** (MT, 1 μM), **LysoTCM** (LT, 1 μM), non-targeted **TCM alkyne** (NT, 1 μM), or NaSH (HS^-, 1 μM). Cell viability was assessed using a CCK-8 kit. Results are expressed as mean ± SD ($n = 12$). ***$p < 0.001$, ****$p < 0.0001$.

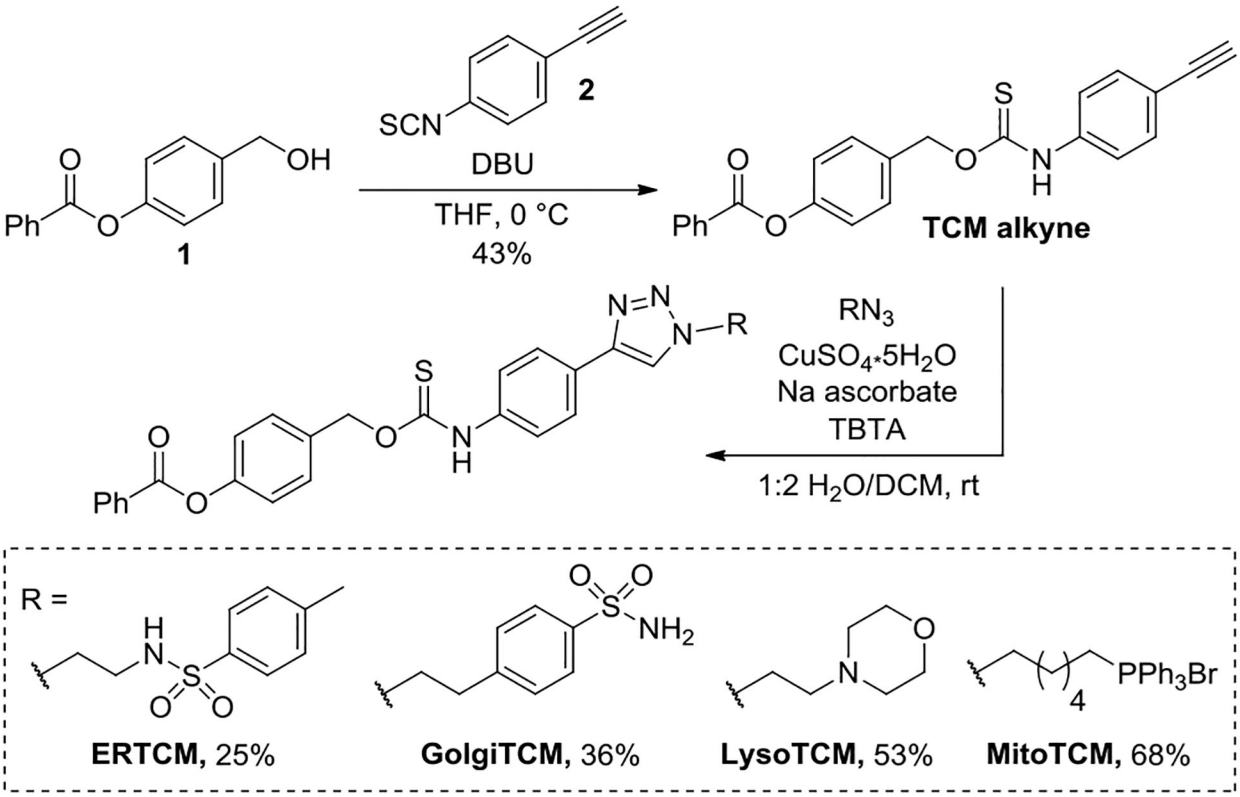

Scheme 1.
Synthesis of organelle-targeted COS/H_2S donors.

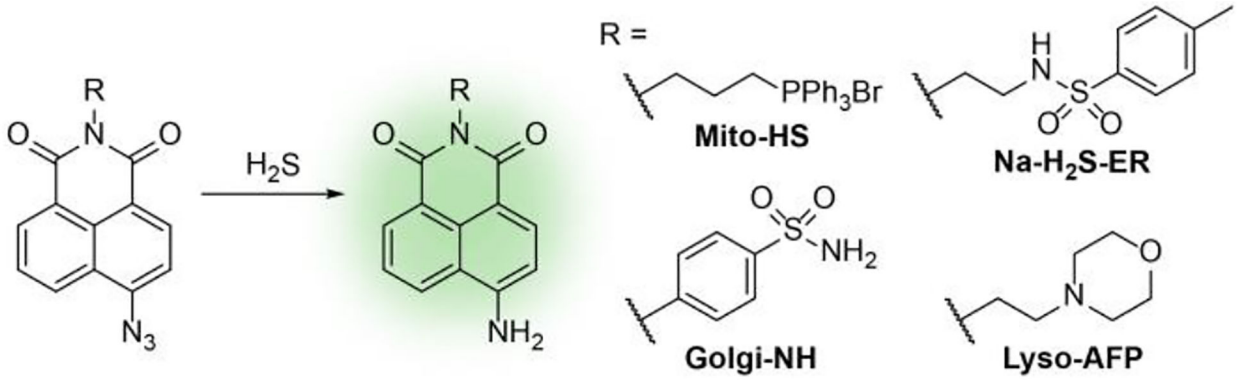

Scheme 2.
Selected organelle-targeted H_2S-responsive fluorescent probes.